SR 219

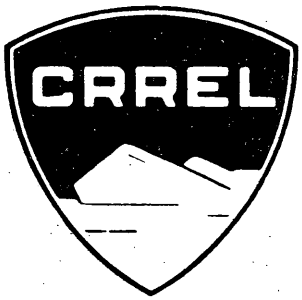


Special Report 219

# SIMULATED SNOWDRIFT PATTERNS

## Evaluation of Geometric Modeling Criteria for a Three Dimensional Structure

Darryl J. Calkins

March 1975

PREPARED FOR
DIRECTORATE OF MILITARY CONSTRUCTION
OFFICE, CHIEF OF ENGINEERS
DA PROJECT 4A162121A894
BY
CORPS OF ENGINEERS, U.S. ARMY
**COLD REGIONS RESEARCH AND ENGINEERING LABORATORY**
HANOVER, NEW HAMPSHIRE

The findings in this report are not to be construed as an official Department of the Army position unless so designated by other authorized documents.

Unclassified

SECURITY CLASSIFICATION OF THIS PAGE *(When Data Entered)*

## REPORT DOCUMENTATION PAGE

READ INSTRUCTIONS BEFORE COMPLETING FORM

| | |
|---|---|
| 1. REPORT NUMBER: Special Report 219 | 2. GOVT ACCESSION NO. |
| 3. RECIPIENT'S CATALOG NUMBER | |
| 4. TITLE *(and Subtitle)*: SIMULATED SNOWDRIFT PATTERNS<br>Evaluation of Geometric Modeling Criteria for a Three Dimensional Structure | 5. TYPE OF REPORT & PERIOD COVERED |
| | 6. PERFORMING ORG. REPORT NUMBER |
| 7. AUTHOR(s): Darryl J. Calkins | 8. CONTRACT OR GRANT NUMBER(s) |
| 9. PERFORMING ORGANIZATION NAME AND ADDRESS: U.S. Army Cold Regions Research and Engineering Laboratory, Hanover, N.H. 03755 | 10. PROGRAM ELEMENT, PROJECT, TASK AREA & WORK UNIT NUMBERS: DA Project 4A162121A894 |
| 11. CONTROLLING OFFICE NAME AND ADDRESS: Directorate of Military Construction, Office, Chief of Engineers, Washington, D.C. 20314 | 12. REPORT DATE: March 1975 |
| | 13. NUMBER OF PAGES: 16 |
| 14. MONITORING AGENCY NAME & ADDRESS *(if different from Controlling Office)* | 15. SECURITY CLASS. *(of this report)*: Unclassified |
| | 15a. DECLASSIFICATION/DOWNGRADING SCHEDULE |

16. DISTRIBUTION STATEMENT *(of this Report)*

Approved for public release; distribution unlimited.

17. DISTRIBUTION STATEMENT *(of the abstract entered in Block 20, if different from Report)*

18. SUPPLEMENTARY NOTES

19. KEY WORDS *(Continue on reverse side if necessary and identify by block number)*

Flumes
Hydraulic models
Model basins
Model tests
Sediment transport
Snowdrifts
Snow removal

20. ABSTRACT *(Continue on reverse side if necessary and identify by block number)*

Simulated drifting snow patterns were examined for a single structure using fine sand and water in a hydraulic flume. Three models of the structure were constructed at different scales and the experimental data revealed that model scale had very little effect on the areal distribution patterns. Flow velocity also had very limited influence on the drift patterns, provided the channel velocity was greater than the threshold velocity of the sand particle. Lengthening the duration of the test runs made it easier to distinguish the patterns but did not

DD FORM 1 JAN 73 1473 EDITION OF 1 NOV 65 IS OBSOLETE

Unclassified

SECURITY CLASSIFICATION OF THIS PAGE *(When Data Entered)*

20.
change their shape. The above experimental data suggest that modeling under the concept of Reynolds number independence is satisfactory.

## PREFACE

This report was prepared by Darryl J. Calkins, Research Hydraulic Engineer, Applied Research Branch, Experimental Engineering Division, U.S. Army Cold Regions Research and Engineering Laboratory. The work was funded under DA Project 4A162121A894, *Engineering in Cold Environments*, Task 20, *Cold Regions Facilities Operations, Maintenance, and Engineering of Military Installations*, Work Unit 003, *Control and Removal of Ice and Snow at Facilities*.

The author would like to thank Dr. George Ashton and L. David Minsk of USA CRREL for their technical review of the manuscript and guidance in performing the experimental work.

## CONTENTS



## ILLUSTRATIONS



## TABLE

# SIMULATED SNOWDRIFT PATTERNS
## Evaluation of Geometric Modeling Criteria for a Three Dimensional Structure

by

Darryl J. Calkins

### Introduction

Modeling of drifting snow conditions around various structures, including buildings, highway sections, etc. has been studied in hydraulic flumes using fine sand[7, 11] and in wind tunnels using borax.[1, 10] Most studies have used a single geometric modeling scale, and there has been little effort to evaluate a range of model scales and their effect on the resulting distribution patterns. This study evaluates, in a hydraulic flume, simulated snowdrift patterns for a three-dimensional model with respect to a) time, b) flow velocity greater than 0.30 m/sec, and c) geometric scale.

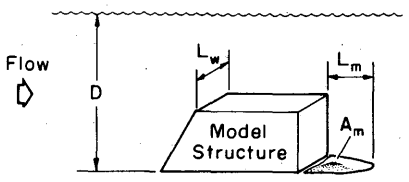


*Figure 1. Three-dimensional view of model structure.*

The model structure represents a radar housing being constructed in North Dakota.[4] Its shape is trapezoidal with three walls vertical and the other at 25° with the vertical (Fig. 1), the inclined face representing the "eye" of the radar beam. The base of the prototype structure is 62 × 65 m and the height is 39.5 m. Three models of the structure were fabricated from clear Plexiglas at scales of 1:200, 1:300 and 1:400.

There are no field data yet available to correlate with the data acquired in this laboratory investigation or to verify the conclusions reached.

### Previous hydraulic modeling work

Theakston[12] and Isyumov[7] used hydraulic flumes with fine Ottawa sand to simulate the drifting snow. Theakston's work followed a qualitative approach, simulating snowdrift patterns around various types of structures from known conditions and determining remedial solutions by trial positioning of snow fences, building realignment or terrain modification. Isyumov, in his study on roof snow loads, used the hydraulic modeling technique to predict the location and deposition of snow on roofs of various shapes, even though he had at his disposal a large atmospheric wind tunnel. His modeling criterion was based on upstream surface roughness conditions for geometric scales, with the fall velocity ratio of the model and prototype snow particles as the velocity scale.

The factors considered in choosing a water and sand system as opposed to a wind tunnel to model drifting snow were as follows: a) the borax/air simulator had problems with particle charging; b) a wind tunnel large enough to simulate atmospheric boundary layers adequately would have been extremely expensive; c) no satisfactory method of handling particulate matter in such a wind tunnel was found, and directors of the large wind tunnel laboratories would not introduce any particulate

The ratios of terminal fall velocity for sand in water and snow in air range between 1/18 and 1/36; typical ratios of threshold shear velocities for sand and new dry snow[7] are also in the same range: 1/18 to 1/44. Therefore a velocity scale between 1/10 and 1/50 would appear to be adequate for proper model representation due to the wide range of reported shear and terminal fall velocities for snow particles. Relaxation of the Densimetric Froude number for the velocity scale appears not to be an unrealistic decision. The time scale of model events is simply $\lambda_T = \lambda_L/\lambda_V$, which in light of previous experimental work would range anywhere from 1/5 to 1/20, depending on choice of geometric and velocity scales.

**Design of experiment and procedures**

Three models of the radar structure were constructed from Plexiglas at scale ratios $\lambda_L$ of 1:200, 1:300 and 1:400 with physical dimensions approximately 30 × 30 × 18 cm, 20 × 20 × 12 cm and 15 × 15 × 9 cm, respectively. The models were fastened to a circular aluminum plate with an inscribed 2-cm grid system from which measurements of the accumulation patterns could be taken. A camera set-up was later installed for permanent record and ease in interpreting the distribution of sand. The hydraulic flume has an internal cross section of 0.925 × 0.925 m; additional information on its design can be found in ref. 3.

The method used to introduce sand into suspension is similar to a rising platform technique. A 4.5-cm layer of Ottawa F-140 sand (all sand passing the no. 200 sieve removed) was leveled over the entire flume bottom. The flow velocity was then increased until it exceeded the threshold particle velocity, allowing the material to be entrained into the flow. Concentration profiles upstream of the model were measured in each test run using an electro-optical probe. Results and discussion of this phase of the experiment may be found in the Appendix.

The models were aligned with the sloping side facing upstream in all tests; this particular orientation represents snow blowing from the north for this particular structure. Prior to each run, all sand was cleared from the circular plate. The depth of water in the flume was maintained relatively constant for each run at 44-45 cm. Velocity profiles were not obtained because the instrumentation had not arrived at the time of the experiments.

Simulated snowdrift patterns were measured behind each of the models to evaluate the effect of the geometric scale with respect to flow velocity and its duration. The patterns were interpreted from the grid system and photographs. Each time a measurement of the areal distribution was conducted, the velocity had to be decreased or flow completely shut off because the suspension of sand in the flow prohibited visual measurement or photographs from being taken.

**Evaluation of data**

Table I lists the measurements and calculations associated with each model run except for the concentration profiles, which are presented in the Appendix. The initial set of photographs taken to support the data collection were of such poor quality that detailed analysis could not be performed on the sand patterns. Consequently, a different camera, lens and mounting procedure have been developed for all future tests and have proven reliable in photographing the areal distribution patterns.

The data in the three tables are divided into two sections, the measured flow conditions and the areal distribution of the sand. $L_m$ denotes the streamwise length from the center of the leeward edge of the model to the outer limits of the deposition pattern. Figure 1 depicts the configuration of deposition with reference to the model. $A_m$ is the areal extent of the sand pattern and $L_w$ is the model width.

When the average flow velocity was low (0.35 m/sec), but greater than the threshold particle velocity (≈ 0.25 m/sec), the sediment distribution was uniform but low (300-500 ppm) and it took a longer time for the sand formation to develop behind the model. After 40 minutes of flow, the deposition pattern was clearly evident, sufficient material having been deposited on the circular

**Table I. Test results.**

| Test | Duration (min) | Depth (m) | $Q$ ($m^3$/sec) | $V$ (m/sec) | $L_m$ (cm) | $A_m$ ($cm^2$) | $A_m/L_w^2$ | $L_m/L_w$ |
|---|---|---|---|---|---|---|---|---|
| | | | **a. Model scale 1:200, $L_w$ = 30 cm.** | | | | | |
| 1-S200 | 30 | 0.445 | 0.145 | 0.351 | 19 | 404 | 0.44 | 0.63 |
| | 60 | 0.455 | 0.145 | 0.351 | 18 | 348 | 0.38 | 0.59 |
| | 120 | 0.455 | 0.145 | 0.351 | 18 | 380 | 0.41 | 0.59 |
| 2-S200 | 25 | 0.440 | 0.185 | 0.458 | 18 | 328 | 0.36 | 0.59 |
| | 50 | 0.440 | 0.185 | 0.458 | 17 | 346 | 0.38 | 0.56 |
| | 75 | 0.440 | 0.185 | 0.458 | 17 | 340 | 0.37 | 0.56 |
| 3-S200 | 20 | 0.440 | 0.220 | 0.549 | 20 | 318 | 0.35 | 0.67 |
| | 38 | 0.440 | 0.220 | 0.548 | 17 | 362 | 0.39 | 0.56 |
| | 70 | 0.440 | 0.220 | 0.548 | 18 | 376 | 0.41 | 0.59 |
| Average | | | | | 18 | 355 | 0.39 | 0.60 |
| | | | **b. Model scale 1:300, $L_w$ = 20 cm.** | | | | | |
| 1-S300 | 18 | 0.445 | 0.145 | 0.351 | 15 | 171 | 0.42 | 0.74 |
| | 43 | 0.445 | 0.145 | 0.351 | 15 | 174 | 0.43 | 0.74 |
| | 75 | 0.445 | 0.145 | 0.351 | 15 | 187 | 0.46 | 0.74 |
| 2-S300 | 25 | 0.445 | 0.185 | 0.458 | 15 | 174 | 0.43 | 0.74 |
| | 60 | 0.445 | 0.185 | 0.458 | 13 | 142 | 0.35 | 0.64 |
| | 88 | 0.445 | 0.185 | 0.458 | 13 | 174 | 0.43 | 0.64 |
| 3-S300 | 24 | 0.445 | 0.220 | 0.533 | 10 | 140 | 0.34 | 0.50 |
| | 44 | 0.445 | 0.220 | 0.533 | 10 | 139 | 0.34 | 0.50 |
| Average | | | | | 13 | 162 | 0.40 | 0.65 |
| | | | **c. Model scale 1:400, $L_w$ = 15 cm.** | | | | | |
| 1-S400 | 20 | 0.445 | 0.145 | 0.356 | 10 | 90 | 0.39 | 0.66 |
| | 40 | 0.445 | 0.145 | 0.356 | 10 | 106 | 0.46 | 0.66 |
| | 100 | 0.445 | 0.145 | 0.356 | 10 | 89 | 0.39 | 0.66 |
| 2-S400 | 20 | 0.445 | 0.185 | 0.455 | 10 | 110 | 0.48 | 0.66 |
| | 40 | 0.445 | 0.185 | 0.455 | 11 | 103 | 0.45 | 0.66 |
| | 100 | 0.445 | 0.185 | 0.455 | 11+ | 116 | 0.50 | 0.72 |
| 3-S400 | 20 | 0.445 | 0.220 | 0.541 | 10 | 90 | 0.39 | 0.66 |
| | 35 | 0.445 | 0.220 | 0.541 | 9 | 76 | 0.33 | 0.59 |
| | 55 | 0.445 | 0.220 | 0.541 | 10 | 95 | 0.41 | 0.66 |
| Average | | | | | 10 | 96 | 0.42 | 0.66 |

plate. For the higher velocity runs (0.45 m/sec and 0.54 m/sec) the sand pattern was evident after 15-20 minutes of flow, because the concentration of material in suspension had increased significantly and deposition was occurring faster.

Figure 2 is a plan view of the deposition patterns behind the three scale models for three flow velocities. The plotted data for the three models have been reduced to an equivalent scale to allow the simulated drift patterns to be compared. It is evident that little variation occurs in the outlines of the patterns after the flow duration has exceeded 60 minutes, while it was observed that the depth of accumulation was increasing within the eddy zone. Once the eddy zone had been clearly outlined by the depositing material, the extent of the drift did not change significantly. Even when the average flow velocity was increased to 0.53 m/sec the drift pattern was still similar to the patterns measured for the other two flow velocities (Fig. 2). In subsequent tests at velocities lower than the threshold particle velocity, using an overhead sand feed, the areal

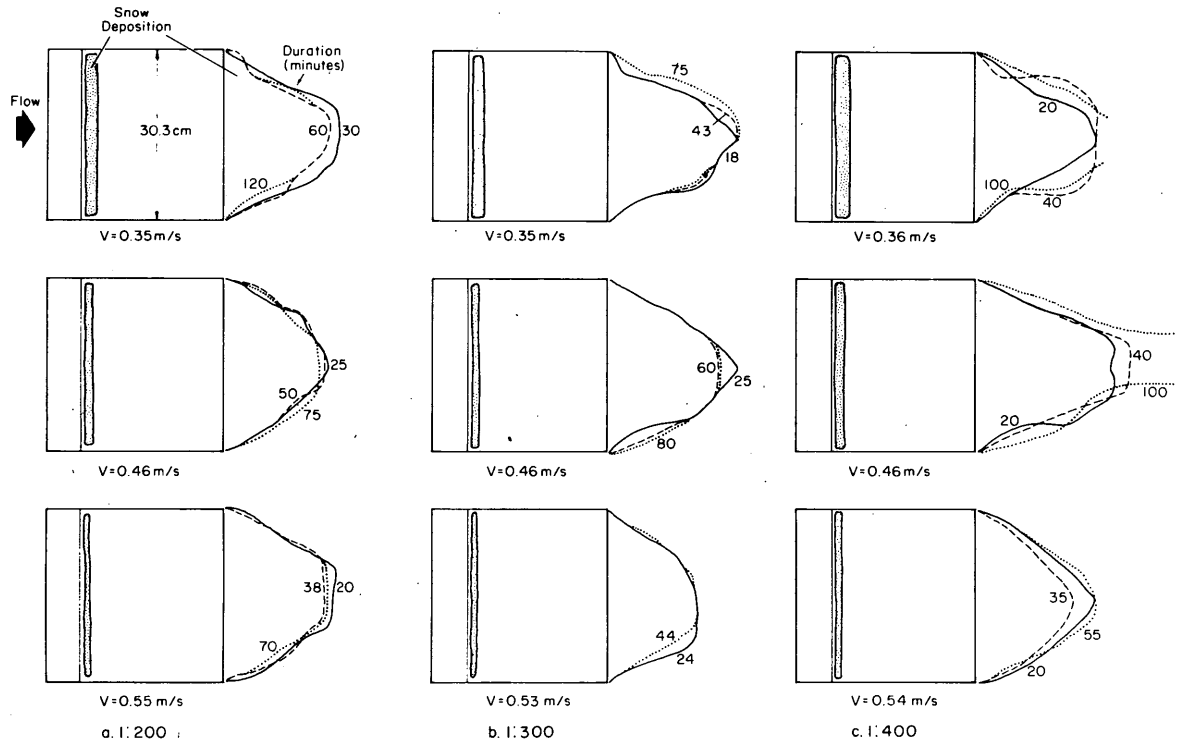


*Figure 2. Simulated snowdrift patterns for all model tests.*

pattern differed slightly behind the center section of the model but remained similar to the pattern in the 1:400 series at a velocity of 0.46 m/sec. This probably indicates that the strength of the shedding vortices is low and that they are unable to completely clean an area behind the model as in the higher velocity runs. This could be considered an early stage of drift development at low velocities, but as seen in the higher velocity flows the parabolic shape will eventually be realized for this particular building configuration.

Finney,[5] in his pioneering work on snowdrift control for highways, found that the eddy area formed behind a particular snow fence was invariant for wind tunnel speeds of 10, 20 and 30 mph. When particulate matter was introduced into the air stream, Finney found:

> "At low wind velocities, the end of the drift terminated at a certain distance from the end of the eddy depending on the amount of snow and wind velocity. As the amount of snow and the wind velocity increased, the end of the drift moved to the end of the eddy and remained near that point. When the drift had completely filled the eddy area, the excess material was carried along the top of the drift and beyond the effective area of the snow fence. This was true only of the horizontal and vertical slat fences. The solid barrier produces a drift that does not extend to the end of the eddy area except under very low wind velocities."

The position of maximum depth was found to be related to the wind speed. At higher wind speeds the point of maximum depth was further from the snow fence than at lower wind speeds, although the end points of the drifts appeared to correspond closely to eddy end points. Based on this preliminary information, it would appear that the eddy zone behind this two-dimensional structure is independent of the free stream velocity for the two cases mentioned previously.

An additional run was conducted to evaluate the effect of increased flow depth on the deposition pattern at a flow velocity greater than the particle threshold velocity. The 1:200 model was

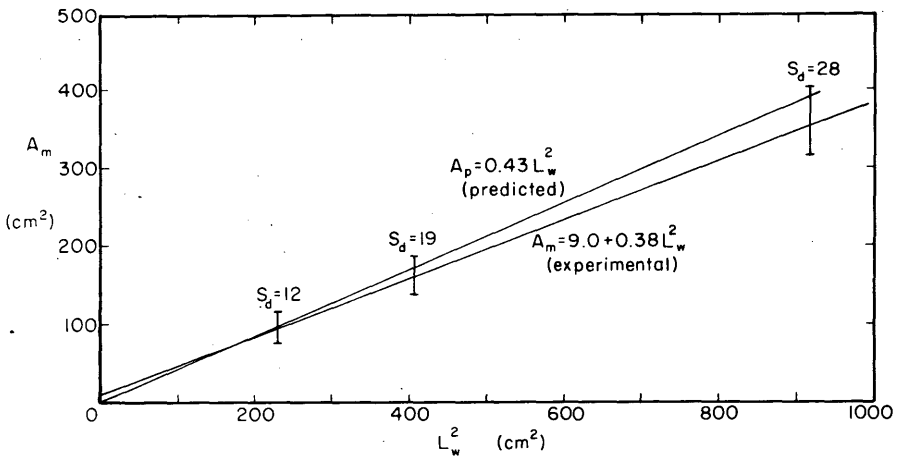


*Figure 3. Areal accumulation versus the square of the model width, measured and predicted.*

used and no visible or measurable differences were noticed in the areal patterns behind the structure. However, additional deposition on the roof was observed.

The areal distribution patterns for all model runs are given in Figure 2 and the data are summarized in Table I. The area of sand behind each of the model structures was relatively constant, with a standard deviation of 28, 19 and 12 $cm^2$ for the 1:200, 1:300 and 1:400 models respectively. Measurement of the areal pattern was referenced to the 2-cm grid pattern and estimated to the nearest centimeter; consequently, measurement errors in the pattern probably contributed to the large range in the data for the area of sand accumulation. The photographs, if they had been usable, would have provided a more accurate means of measurement.

The relationship between the area of sand accumulation and the square of the model building width is shown in Figure 3. From Table I the ratio $A_m/L_w^2$ is nearly the same regardless of the model scale, or flow velocity. The equation of the line in Figure 3 is approximately

$$A_m = 9.0 + 0.38 L_w^2 \tag{3}$$

where $A_m$ = area of accumulation, $cm^2$

$L_w$ = width of model building, cm.

However, forcing the equation through the origin changes the slope only slightly to 0.40, resulting in

$$A_m = 0.40 L_w^2. \tag{4}$$

This implies that the sand pattern or simulated snowdrift is proportional to the square of the building width when flow is normal to the sloping face. Since the ratio $A_m/L_w^2$ remained essentially constant regardless of geometric scale, it implies that the physical dimensions of the models studied were acceptable. This also suggests that blockage effects are not significant for a model width up to 30 cm in a 92-cm-wide hydraulic flume.

It appears that the shape of the simulated snowdrift can be approximated by a parabola if the ratio $(L_m/L_w)$ is known. The shape function takes the form

$$A_p = \frac{2}{3} L_m L_w \tag{5}$$

where $A_p$ = area, $cm^2$

$L_m$ = distance from the leeward edge of the model at the center to outside edge of the drift, cm

$L_w$ = model width, cm.

The ratio of $L_m/L_w$ was calculated for each run and averaged for each model scale studied (Table I). Assuming an average value of 0.64 and substituting into eq 5 for $L_m$ yields

$$A_p = 0.43 L_w^2. \tag{6}$$

Equation 6 predicts an area of sand accumulation only slightly greater than that predicted by eq 3 or 4, but within the range of the data points (Fig. 3). Model scale did not appear to influence the results significantly although a slight increase in the ratio $L_m/L_w$ with respect to decreasing model size was noticed, as shown in the table of calculations; this could be due to the limited accuracy of the initial data.

**Discussion of scaling criteria**

Three model geometric scales $\lambda_L$ (1:200, 1:300 and 1:400) were evaluated for areal changes in snow deposition patterns at three separate velocity scales. Assuming that the threshold velocity 2 m above the snow surface ranges from 4-10 m/sec, the velocity scales $\lambda_V$ range from 1/16 to 1/40 for an average flume velocity of 0.25 m/sec, the threshold flow velocity for the sand particles. Since model snow depths were not measured and prototype measurements are not available, a check on the time scale could not be performed.

Within the range of model geometric scales studied, 1:200 to 1:400, and using flow velocities greater than the threshold velocity of 0.25 m/sec, the areal pattern of snow deposition did not change significantly. An average flow Reynolds number for this series of experiments would be $1.8 \times 10^5$, well within the range previously reported. Two conditions are implied: 1) the velocity scale has little effect on pattern distribution, and 2) the Reynolds number independence criterion is upheld for sediment-laden flows in these model studies, and is likewise implied by Finney's results in his study of model snow accumulations for snow fences.

Using the scale ratio of either shear or fall velocities as the proper velocity scale $\lambda_V$ appears more appropriate than using the densimetric Froude number relationship. The densimetric Froude number exaggerates the particle to fluid density difference whereas the fall velocities of the particles in their respective fluids appear to be a better representation of the velocity characteristics. Likewise the threshold shear velocities in both model and prototype systems are within the same velocity scale range as the fall velocity relationships.

With the data suggesting Reynolds number independence for modeling conditions and an aerodynamically rough flow established in the model flow field, the use of $(Z_0)_m/(Z_0)_p$ as the choice for a proper geometric scale appears to be satisfactory at this point in our studies. The velocity scale relationship also appears to be best defined by considering the fall or shear velocity properties of the particles. The one major drawback in our validation program is accurate time-related snow accumulations for field structures and the relation to meteorological conditions. Recently time-accumulation measurements for snow fences were made available to CRREL and a check on the velocity scale corresponding to the proper time increments can be analyzed in these model studies.

## Conclusions

Three models of the same structure were constructed at 1:200, 1:300 and 1:400 scale. The extent of sand accumulation patterns behind these models with the sloping face placed normal to the flow was proportional to the square of the model width when the flow velocity was greater than the particle threshold velocity. The shape of the areal accumulation pattern was closely fitted to a parabola $A_p = 0.43\ L_w^2$ while the actual measured area function was $A_m = 9.0 + 0.38\ L_w^2$, nearly passing through the origin. Using geometric scales 1:200 to 1:400 and velocity scales between 1/16 and 1/40 resulted in snow deposition patterns that were nearly identical. The data suggest that the choice of geometric scale is not that critical nor is the exact flow velocity scale, thereby supporting the concept of Reynolds number independence for modeling.

## Literature cited

1. Brier, F.W. (1972) Snowdrift control techniques and procedures for polar facilities. Naval Civil Engineering Laboratory Technical Report 767.

2. Budd, W. et al. (1966) Studies in Antarctic meteorology, The Byrd snow drift project – Outline and basic results (Mortin J. Rubin, Editor). Antarctic Research series, vol. 9.

3. Calkins, Darryl (1974) A research hydraulic flume for modeling drifting snow: Design, construction and calibration. U.S. Army Cold Regions Research and Engineering Laboratory (USA CRREL) Technical Report 251.

4. Cohen, Edward and E.B. Laing (1973) Radar building can withstand nuclear attack. *Civil Engineering*, ASCE, vol. 43, no. 10, p. 46-50.

5. Finney, E.A. (1934) Snow control on the highway. Michigan State College, Experiment Station Bulletin no. 57.

6. Hubbard Instrument Company (1970) Operation manual for electro-optical probe. Iowa Institute of Hydraulic Research.

7. Isyumov, Nicholas (1971) An approach to the prediction of snow loads. Ph.D. Dissertation to the Faculty of Engineering Science, The University of Western Ontario, London, Ontario, Canada.

8. Mellor, Malcom (1965) Blowing snow. USA CRREL Cold Regions Science and Engineering Monograph III-A3c.

9. Rouse, Hunter (1950) *Engineering hydraulics*. New York: John Wiley and Son.

10. Snyder, William (1972) Similarity criteria for the application of fluid models to the study of air pollution meteorology. *Boundary Layer Meteorology*, vol. 3, no. 1, Sept.

11. Strom, G.H. et al. (1962) Scale model studies on drifting snow. U.S. Army Snow, Ice and Permafrost Research Establishment (USA SIPRE) Research Report 73.

12. Theakston, F.H. (1970) Model techniques for controlling snow on roads and runways. HRB Symposium, Snow Removal and Ice Control Research, Hanover, N.H., Special Report 115.

# APPENDIX

The electro-optical probe built by the Hubbard Instrument Company was calibrated in the laboratory for the sand used in the experimental studies. A 1000-ml beaker was filled with water and agitated by a magnetic stirrer; 1-g increments of sand were added and yielded the calibration curve shown in Figure A1.

The Ottawa sand (F-140) used in the experiments had the following gradation analysis.

| Sieve size | Percent retained |
|---|---|
| 70 | 2 |
| 100 | 12 |
| 140 | 49 |
| 200 | 37 |

The amount of material in suspension was measured for each run using the concentration probe. Figure A2 shows the concentration profiles for the 1:300 model tests for two flow velocities, 0.35 and 0.46 m/sec. Figure A3 is a similar graph expressing snow transport as a function of height. Remarkable similarities exist between the two figures. At low flows there is relatively uniform distribution except very near the bed surface where the amount of material in suspension increases significantly. At the higher velocities the curves still retain their shape but more material is entrained, resulting in higher concentrations.

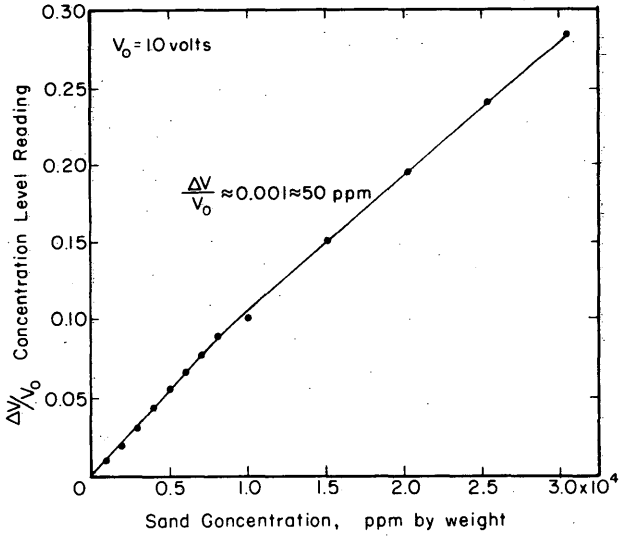


*Figure A1. Sediment concentration probe calibration.*

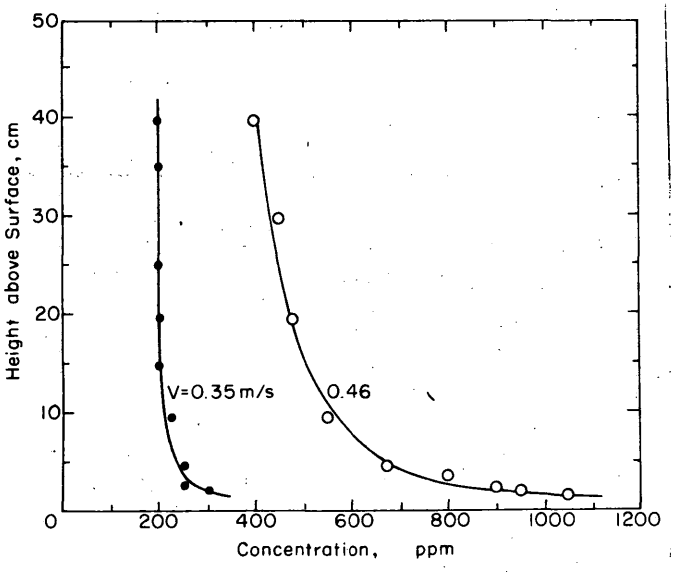


*Figure A2. Typical sediment concentration profiles at 0.35 and 0.46 m/sec.*

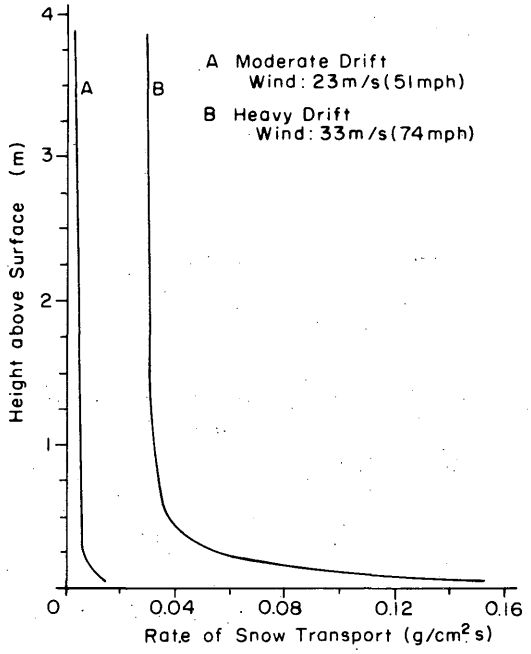


*Figure A3. Snow transport profile at Byrd Station. (From Mellor.[8])*

The sediment discharge per unit width for a two-dimensional flow is given by the integral

$$q_s = \int_0^y c(y)\,u(y)\,dy$$

where $u(y)$ is the velocity distribution, $c(y)$ is the concentration distribution and $y$ is the depth of flow. The above integral can be solved, as the concentration probe measures the sediment distribution function and the velocity distribution can be measured using a current meter.

The fundamental equation of sediment suspension found in most texts presumes a condition of equilibrium to exist between the rate at which the particles fall under their own weight and the rate at which they are entrained. Using von Karman's logarithmic velocity law to obtain the distribution of the diffusion coefficient, one may derive the well known equation for two-dimensional flow (Rouse[9]):

$$C = C_a \frac{y - z}{y - a} \frac{a}{z}^{w/ku^*} \qquad \text{(A1)}$$

where $a$ = reference level

$C_a$ = concentration at reference level

$C$ = concentration at depth $z$

$z$ = depth from bottom to a point measurement

$y$ = depth of flow

$w$ = fall velocity

$k$ = von Karman's constant

$u^*$ = friction velocity.

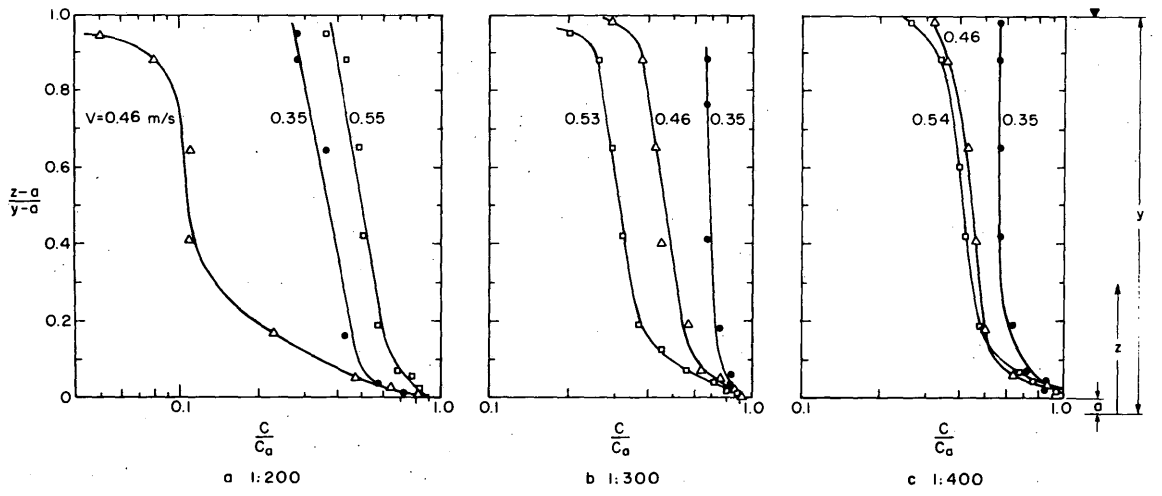


*Figure A4. Relative sand concentration profiles. a. 1:200 model. b. 1:300 model. c. 1:400 model.*

The value of a chosen for all experimental runs was 1 cm above the bed surface. The relative distribution of sediment suspension characteristics for all model tests at a depth of 44.5 cm is given in Figure A4. Figures A4b and c show the general trend; increased flow velocity over the sand bed caused more material to be picked up and kept in suspension. The data in Figure A4a for the 1:200 model tests appear to be erratic. Possibly the zero control was accidentally disturbed during the experiment, giving improper voltage readings. The family of curves in Figure A4 represent various values of $w/u^*$ ($u^* = \sqrt{\tau/\rho}$) which are given in Figure A5. The range of values for $w/u^*$ (0.08-0.12) in the experimental runs shows a sand with uniformity of concentration above 10-15% of the total depth of flow, the coarser sand particles being restricted to the lower 10% of the depth, as indicated by the break in the data points. Rouse[9] also implies this same reasoning.

Similar snow concentration profiles have been plotted from the data collected by Budd et al.[2] in the Antarctic (Fig. A6). An assumption was made regarding the depth of the flow $y$: it was chosen as the height of the highest concentration measurement ($y = 4$ m), and the reference level was selected as the lowest measurement. From Figure A6 the low value of $y$ chosen reflects that a relatively uniform concentration wasn't achieved, but if measurements had been made at greater heights, the uniformity would be present and the curve wouldn't appear to be skewed to the left. The plot in Figure A6 does show that the majority of snow particles being transported are near the surface.

Snow deposition on the roof was more evident in the test runs on the 1:200 model than on the other two models. Although the experiment was not designed for studying snow accumulation on roofs, it should be noted why the patterns were not clearly evident on the other models. Since the velocity profile was not measured for any of the experiments, the boundary layer thickness $\delta$ can only be estimated. Izyumov measured the boundary layer thickness over several bed roughnesses with an average value of 0.12 m. Assuming the seventh root velocity profile and the stress expression for turbulent pipe flow, the resulting equation from Rouse[9] is used to calculate the boundary layer thickness in a turbulent flow:

$$\delta_x = \frac{(0.38)x}{R_x^{0.2}} \qquad \text{(A2)}$$

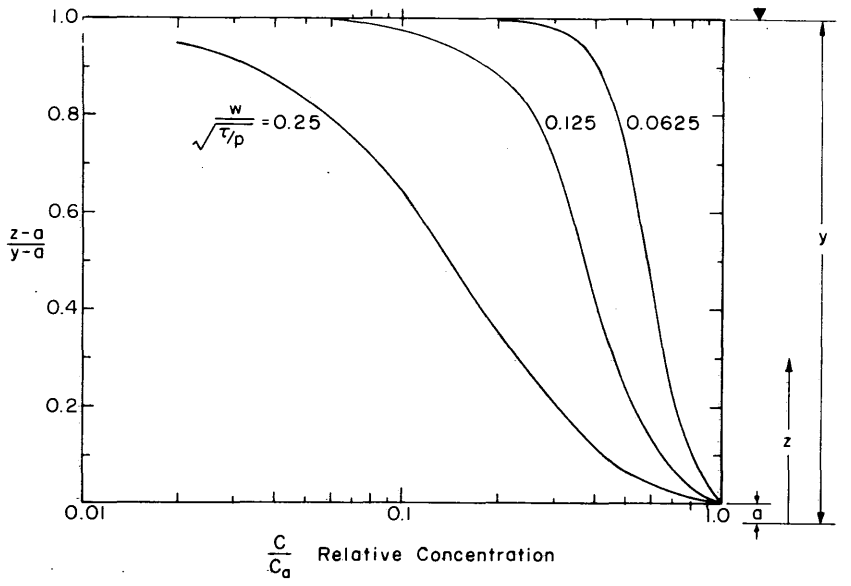


*Figure A5. Theoretical relative concentration profiles. (From Rouse.[9])*

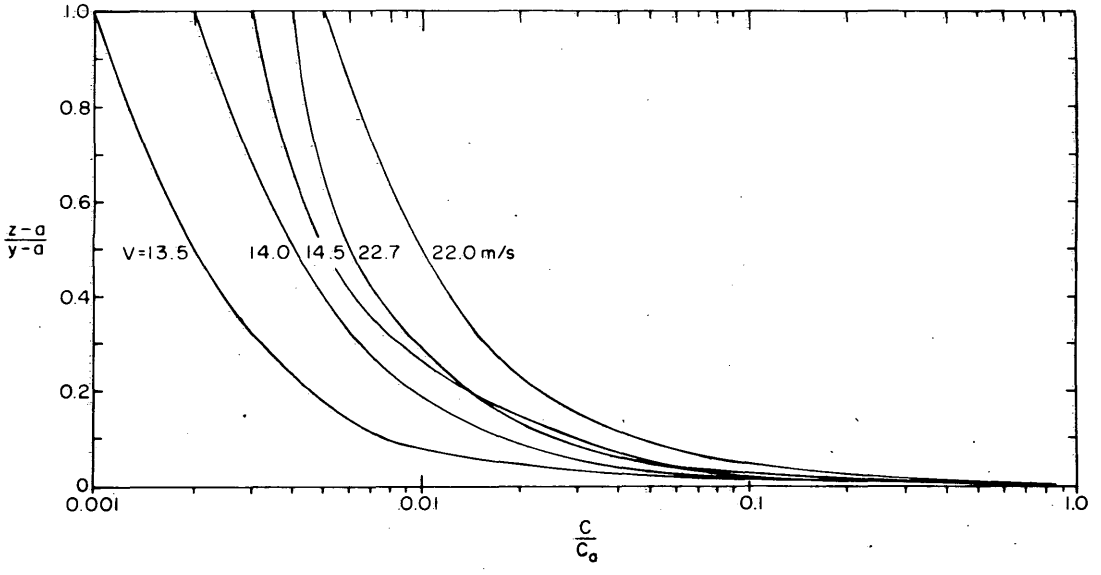


*Figure A6. Relative snow concentration profiles at Byrd Station. (From Budd et al.[2])*

where $\delta_x$ = boundary layer thickness

$x$ = distance downstream

$R_x$ = Reynolds no. = $V_0 x/\nu$

$V_0$ = flow velocity

$\nu$ = kinematic viscosity.

For average conditions in our flume using $V_0$ = 0.45 m/sec, $x$ = 4.6 m, $\nu = 1.13 \times 10^{-6}$ m$^2$/sec, the boundary layer thickness = 0.09 m.

If the height of the model is less than or equivalent to the boundary layer thickness $\delta$, a proper flow profile over the roof of the structure might not be achieved. The heights of the 1:300 and 1:400 models were 0.12 and 0.09 m, clearly very near the displacement thickness calculated above and as measured by Isyumov.[7] One can only assume that this might be one reason for sand deposition not showing very clearly on these smaller scale models. When the flow depth was increased from 45 to 72 cm with the 1:200 model, the increased sand deposition on the roof was clearly evident. Tests were not conducted for the other models at the deeper flow depths. Isyumov[7] has found that terrain roughness has a significant effect on snow deposition on roofs, and further analysis should reflect this parameter in studies of drifting snow around various structures.